Available online at www.sciencedirect.com
ScienceDirect
International Journal of Pavement Research and Technology 9 (2016) 169–177
www.elsevier.com/locate/IJPRT

# Prediction of autogenous shrinkage of concretes by support vector machine

Jun Liu, KeZhen Yan *, Xiaowen Zhao, Yue Hu

*College of Civil Engineering, Hunan University, Changsha 410008, Hunan, China*

Received 2 December 2015; received in revised form 12 June 2016; accepted 13 June 2016
Available online 18 June 2016

**Abstract**

Support vector machine (SVM) is firmly based on learning theory and uses regression technique by introducing accuracy insensitive loss function. In this paper, a SVM model for the autogenous shrinkage of concrete mixtures was proposed. The model chose water-to-cementitious material ratio (w/cm), cement content, silica fume percentage, fly ash percentage, total aggregate content, curing temperature, high-range water-reducing admixture (HRWRA) content, and hydration age as input parameters, and the autogenous shrinkage of concrete as the model output. The data set used for training and testing of the SVM model covers the experimental data presented in the existing literature. The developed SVM model was validated using experimental work. The SVM model was compared with the ANN prediction model, the SVM model shows comparable prediction accuracy and could easily be established. In short, the proposed SVM model exhibited excellent capability in predicting the autogenous shrinkage of concrete mixtures.


*Keywords:* Support vector machine; Autogenous shrinkage; Prediction; Concrete mixtures

## 1. Introduction

Concrete is the most widely used construction material worldwide. In the past decades, great efforts have been made to develop a new generation of concrete to improve its performance and competitiveness as a construction material. Consequently, concrete with high performance and high durability has been developed and is used much frequently to construct civil infrastructures. Although such concrete has improved properties, it appears to have an increased tendency to develop early age cracking caused by autogenous shrinkage due to the use of rather low water-to-cementitious material ratio (w/cm) [1]. Cracking in concrete members reduces the load-carrying capacity of the structure. Cracks allow water and other potentially aggressive species, such as deicing salt, chlorides, sulfates, freezing water, $CO_2$, to go through the cover layer to come into contact with the reinforcements, leading to reinforcement corrosion and rupture in steel reinforced concrete [2,3].

Autogenous shrinkage was first mentioned by Lyman in 1934 [4]. For many years, there was little known research conducted on this phenomenon. Since the early 1990s, the importance of autogenous shrinkage has been wholly reconsidered, and now a number of researchers continue to conduct studies on this increasingly important phenomenon [5–8]. Autogenous shrinkage is a deformation caused by the continued hydration of cement, exclusive of the effects of applied load and change in either thermal condition or moisture content [9]. Thus, the measurement of autogenous shrinkage has to be conducted under sealed conditions to eliminate moisture exchange. Autogenous shrinkage of concrete increases as the water-to-

* Corresponding author.
*E-mail address:* yankz@hnu.edu.cn (K. Yan).
Peer review under responsibility of Chinese Society of Pavement Engineering.

http://dx.doi.org/10.1016/j.ijprt.2016.06.003
1996-6814/© 2016 Chinese Society of Pavement Engineering. Production and hosting by Elsevier B.V.

cementitious material ratio (w/cm) decreases. According to Aitcin et al. [10], the autogenous shrinkage will not be high if the w/cm ratio is greater than about 0.42, but will develop rapidly if the w/cm ratio is lower than 0.42. At a very low w/cm ratio of 0.17, an autogenous shrinkage of $700 * 10^{-6}$ for concrete was reported [11]. There are several factors influencing the evolution of the autogenous shrinkage of concrete, including the w/cm [7], curing temperate [11], aggregate content, cement content [12], and the type and percentage of supplementary cementitious materials [7]. These parameters are highly correlative and play complex, combined roles on the development of autogenous shrinkage.

Previous approaches for development of the predictive drying shrinkage models [13–17] do not normally perform well for autogenous shrinkage of concretes with high performance and high durability, they are limited to concretes with relatively low 28-day compressive strengths. In terms of prediction of the early-age autogenous shrinkage of concrete, Nehdi and Soliman [18] have proposed an artificial neural network (ANN) model. However, the ANN has slow convergence speed and poor generalizing performance, and sometimes experiences over-fitting problems. Furthermore, there is no proper method to determine the number of hidden layers. The support vector machine (SVM) is a novel and efficient approach to improve generalization performance and can attain a global minimum. SVMs achieve good generalization ability by adopting a structural risk minimization induction principle that aims at minimizing a bound on generalization error of a model rather than minimizing the error on the training data only. It has ability to avoid overtraining, and has better generalization capability than ANN model. Moreover, the SVMs can always be updated to get better results by presenting new training examples as new data become available [19].

Some of SVM applications in the civil engineering problems include remote sensing images analysis and rainfall-runoff model [20], conceptual cost estimates in construction projects [21], soil moisture prediction [22], slope reliability analysis [23], settlement study of shallow foundations [24], model for contractor prequalification [25], and seismic liquefaction assessment [26].

This paper is the first one to demonstrate the potential of SVM application to predict the autogenous shrinkage of similar concrete mixtures. In this study, the theory and procedure of SVM were briefly reviewed, and training process of the SVM was described. Moreover, the developed SVM model was validated using experimental work.

## 2. Support vector machine

SVM is one of the machine learning (ML) techniques derived from statistical learning theory by Vapnik and Chervonenkis [27]. The foundations of SVM were developed by Vapnik [28] at AT&T Bell Laboratories. Overall, SVMs have been applied in statistics, computer science, and other fields with great success.

In the following, a brief description of the principles of SVMs is provided. One can find more details about statistical learning theory and SVMs in Gunn (1998) and Smola and Scholkopf (2004) [29,30].

Suppose that the training data are given as $\{(x_1, y_1), \ldots, (x_n, y_n)\} \subset X$, where $X$ denotes the space of the training data patterns (e.g., $\boldsymbol{X} = R^d$). $n$ denotes the size of the training data set, $x_i$ denotes the value of the input and $y_i$ denotes the value of output. The goal of SVM is to find a function $f$ that has at most $\varepsilon$ deviations from the actually obtained targets $y_i$ for all the training data, and is also as flat as possible. The functions $f$ for given training data can be represented by the following equation:

$$f(x) = \langle \omega, x \rangle + b \tag{1}$$

where $\omega \subset X$ and $b \subset R$; $<, >$ denote the dot product in $\boldsymbol{X}$; $\omega$ is the weight vector; b is the scalar threshold.

Following statistical theory, SVM determines the regression function by minimizing an objective function. The parameters $\omega$ and $b$ of the regression function are estimated by minimizing the regularized risk function as follows:

Minimize

$$\frac{1}{2}||\omega||^2 + C\sum_{i=1}^{n}(\xi_i + \xi_i^*) \tag{2}$$

Subject to

$$\begin{Bmatrix} y_i - \langle \omega, \varphi(x) \rangle - b \leqslant \varepsilon + \xi_i \\ \langle \omega, \varphi(x) \rangle + b - y_i \leqslant \varepsilon + \xi_i^* \\ \xi_i, \xi_i^* \geqslant 0, \quad i = 1, 2 \ldots l \end{Bmatrix} \tag{3}$$

where $C$ = prespecified SVM tolerance parameter and $\xi_i$ and $\xi_i^*$ = slack variables determining the degree to which data points will be penalized if the error is larger than precision parameter $\varepsilon$. $\varepsilon$ is the insensitive loss function. Fig. 1 illustrates $\varepsilon$–insensitive loss function setting to given data in SVM, and it is also represented by the following equation:

$$L_\varepsilon(y) = \begin{cases} |f(x) - y| - \varepsilon & , |y - f(x)| \geqslant \varepsilon \\ 0, & \text{otherwise} \end{cases} \tag{4}$$

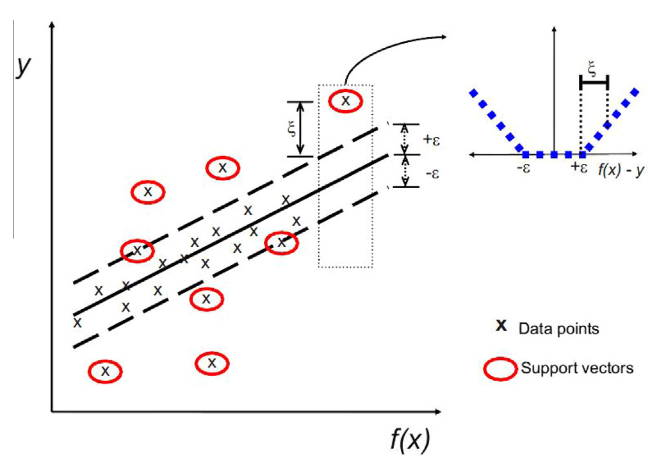


Fig. 1. $\varepsilon$ -insensitive loss function setting for SVM in regression [31].

By introducing Lagrangian multipliers and maximizing, the dual optimization problem can be expressed as: Maximize

$$-\varepsilon\sum_{i=1}^{n}(\alpha_i+\alpha_i^*)-\frac{1}{2}\sum_{i,j=1}^{n}(\alpha_i-\alpha_i^*)(\alpha_j-\alpha_j^*)<x_i,x_j>+\sum_{i=1}^{n}(\alpha_i-\alpha_i^*)y_i \quad (5)$$

Subject to

$$\begin{cases}\sum_{i=1}^{n}(\alpha_i-\alpha_i^*)=0,\\ 0\leqslant\alpha_i,\alpha_i^*\leqslant C, i=1,2,3\ldots n\end{cases} \quad (6)$$

where $\alpha_i, \alpha_i^*$ are called Lagrangian multipliers. Solving Eq. (5) with constraints in Eq. (6) determines the Lagrange multipliers $(\alpha_i, \alpha_i^*)$, and the $w$ and $b$ of regression function given by Eq. (1) are finally obtained as follows:

$$\omega=\sum_{i=1}^{n}(\alpha_i-\alpha_i^*)x_i, \text{Thus}, f(x)=\sum_{i=1}^{n}[(\alpha_i-\alpha_i^*)<x_i,x>]+b \quad (7)$$

$$b=\frac{1}{n}\sum_{i=1}^{n}\left(y_i-\sum_{j=1}^{n}(\alpha_j-\alpha_j^*)<x_i,x_j>\right) \quad (8)$$

Based on the Karush–Kuhn–Tucker (KKT) conditions for quadratic programing, only a small number of coefficients $(\alpha_i-\alpha_i^*)$ will be assumed to have nonzero values (the data points lying on or outside the ε bound have nozero value), and their data points could be referred to as support vectors (see Fig. 1).

In terms of nonlinear regression, instead of trying to fit a nonlinear model, the data are mapped into a high feature dimension space. Therefore, the dot product $<x_i,x_j>$ can be changed into $<\phi(x_i),\phi(x_j)>$ for the nonlinear case. The SVM training algorithm would only depend on the data through dot products in high feature dimension space. Besides, in high feature dimension space, the dot products can be replaced by the kernel function (i.e. $K(x_i,x_j)=<\phi(x_i),\phi(x_j)>$), we only need to use $K$ in the SVM training algorithm without treating the feature space explicitly to obtain the specific formulation of $\phi$. So Eqs. (5)–(7) can be transformed into the following formulation:

Maximize

$$-\varepsilon\sum_{i=1}^{n}(\alpha_i+\alpha_i^*)-\frac{1}{2}\sum_{i,j=1}^{n}(\alpha_i-\alpha_i^*)(\alpha_j-\alpha_j^*)K(x_i,x_j)+\sum_{i=1}^{n}(\alpha_i-\alpha_i^*)y_i \quad (9)$$

Subject to

$$\begin{cases}\sum_{i=1}^{n}(\alpha_i-\alpha_i^*)=0,\\ 0\leqslant\alpha_i,\alpha_i^*\leqslant C, i=1,2,3\ldots n\end{cases} \quad (10)$$

$$f(x)=\sum_{i=1}^{n}[(\alpha_i-\alpha_i^*)K(x_i,x_j)]+b \quad (11)$$

There are four standard conversion of Kernel function mostly used in regression and modeling including:

(1) Linear Kernel.

$$K(u,v)=<u,v> \quad (12)$$

(2) Polynomial Kernel.

$$K(u,v)=<u,v>^d$$
$$K(u,v)=(<u,v>+1)^d \quad (13)$$

Usually the second Kernel is preferred; because it solves the problems of Hessian so as to close zero.

(3) Radial Basis Function (RBF).

$$K(u,v)=\exp(-gamma|u-v|^2) \quad (14)$$

(4) Sigmoid Kernel.

$$K(u,v)=\tanh(-\alpha<u,v>+\mathrm{c}) \quad (15)$$

The kernel parameters should be carefully chosen as they are important to define the high-dimensional feature space and control the complexity of the final solution. The SVMs are largely characterized by the type of its kernel function, it is important to choose the appropriate kernel function and kernel parameters for each application problem in order to guarantee satisfactory results. The kernel-specific parameters were chosen by a trail–and-error approach.

## 3. Development of SVM-based autogenous shrinkage predictive models

### 3.1. Database

As mentioned previously, autogenous shrinkage of concrete has not been researched as extensively as drying shrinkage. To avoid some complexity, only experimental data having mixture components with comparable physical and chemical properties were identified for the training and testing of the SVM. A number of data sets (approximately 518 data points) were selected from different studies, as summarized in Table 1. Moreover, the data are divided into three subsets: training, validation, and testing. The training data are used to train the model to recognize the patterns between input and output data. The validation data are used to evaluate the effectiveness of the developed model in generalizing the underlying relationships and achieving good performance when new data are introduced. The final model is tested with the testing data set, not presented to the model before, to ensure that predictions are real and not artifacts of the training process [18]. Before training, both data sets were normalized within the range of 0.1–0.9 in accordance with the following equation. This preprocessing step increases the efficiency of the SVM training.

Table 1
Database sources and range of input and output variables.

| Source | No. of mixtures | Variables | Maximum | Minimum | |
|---|---|---|---|---|---|
| 1 | Zhang et al. [7] | 9 | Cement, kg/m$^3$ | 924 | 292 |
| 2 | Igarashi et al. [34] | 4 | | | |
| 3 | Yang et al. [35] | 3 | w/cm | 0.6 | 0.24 |
| 4 | Lee et al. [36] | 4 | | | |
| 5 | Akcay and Tasdemir [37] | 1 | SF, % cementitious material | 15 | 0 |
| 6 | Sah and Sato [38] | 1 | | | |
| 7 | Mazloom et al. [39] | 4 | FA, % cementitious material | 35 | 0 |
| 8 | Akkaya et al. [40] | 3 | | | |
| 9 | Bentur et al. [41] | 1 | TA, % total mass | 68 | 30 |
| 10 | Cusson and Hoogeveen [42] | 1 | | | |
| 11 | Jiang et al. [8] | 5 | HRWRA, % cementitious material | 5 | 0.1 |
| 12 | Yoo et al. [43] | 5 | | | |
| 13 | Yun et al. [44] | 4 | Temperature, °C | 35 | 5 |
| | | | Age, h | 363 | 2 |
| | | | Autogenous shrinkage, με | 804.38 | −38.3 |

Notes: TA is total aggregate content; SF is silica fume; FA is fly ash; and HRWRA is high-range water-reducing admixture.

$$x_{\text{normalized}} = \frac{x_i - x_{\min}}{x_{\max} - x_{\min}} \times 0.8 + 0.1 \tag{16}$$

where $x_{\text{normalized}}$ = normalized value of each parameter; $x_i$ = actual value of each parameter; and $x_{\min}$ and $x_{\max}$ = minimum and maximum values of each parameter. For SVM training, eight input variables were selected: water-to-cementitious material ratio (w/cm), cement content, silica fume percentage, fly ash percentage, total aggregate content, curing temperature, HRWRA content, and hydration age. The autogenous shrinkage of concrete was the single output.

### 3.2. Model development

As mentioned above, the data are divided into three subsets: training, validation, and testing. Because there is no precise method for partitioning the database, the SVM model was trained with randomly selected 50% of the total database, while 25% was used for validation and the other 25% for testing. In the training process, the coefficient of determination ($R^2$), the standard error of predicted values divided by the standard error of measured values ($S_e/S_y$), and the root-mean-squared error ($RMSE$) were used as the main criteria to evaluate the performance of the SVM model. Definitions of these evaluation criteria are provided in Table 2. The $R^2$ is a measure of correlation between the predicted and the measured values and therefore, determines accuracy of the fitting model (higher $R^2$ equates to higher accuracy). The $S_e/S_y$ and the $RMSE$ indicate the relative improvements in accuracy and thus a smaller value is indicative of better accuracy. A set of criteria presented in Table 3, originally developed by Pellinen [32], were also adopted in this evaluation.

One of the important steps in SVM model development was the setting up of the appropriate Kernel function $K$, parameters $C$ and ε for training the SVM. In this study, considering the good performance under general smoothness assumptions, the Radial Basis Function (RBF) is used as the kernel function of the SVMs. Consequently, they are especially useful if no additional knowledge of the data is available. This is also demonstrated in the experiment by comparing the results obtained using the RBF with results obtained using the polynomial kernel. The polynomial kernel gives inferior results and takes a longer time in the training of SVMs. The *gamma*, parameters $C$ and ε were chosen by a trial and error approach. The choice of *gamma* = 6; $C = 100$ and $\varepsilon = 0.005$ in this study is because these values produced the best possible results according to the validation set. The software used in this study is "$SVM_{\text{dark}}$".

### 3.3. Sensitivity of predictions to SVM parameters

Sensitivity analysis of SVM control parameters ($C$, ε and *gamma*) on the $R^2$ of the SVM based predictive autogenous shrinkage models was investigated. Fig. 2a gives the $R^2$ of SVMs at various *gamma*, in which $C$ and ε are, respectively,

Table 2
The performance evaluation parameters of concretes autogenous shrinkage prediction model merits.

| Statistical parameters | $R^2$ | $Se/Sy$ | $RMSE$ |
|---|---|---|---|
| Definitions | $R^2 = 1 - \frac{\sum_{i=1}^{n}(y_i^t - y_i^p)^2}{\sqrt{\sum_{i=1}^{n}(y_i^t - \overline{y_i^t})^2}}$ | $\frac{S_e}{S_y} = \sqrt{\frac{\left[\sum_{i=1}^{n}(y_i^t - y_i^p)^2\right] \times n}{\left[\sum_{i=1}^{n}(y_i^t - \overline{y_i^t})^2\right] \times (n-p)}}$ | $RMSE = \sqrt{\frac{1}{n}\sum_{i=1}^{n}(y_i^t - y_i^p)^2}$ |

Note: $y_i^t$ and $y_i^p$ =target and predicted modulus values, respectively, and $\overline{y_i^t}$ and $\overline{y_i^p}$ =mean of the target and predicted modulus values corresponding to $n$ patterns.

Table 3
Statistical criteria for correlation between the observed and the predicted [32].

| Criteria | $R^2$ | $Se/Sy$ |
|---|---|---|
| Excellent | ⩾0.9 | ⩽0.35 |
| Good | 0.79–0.89 | 0.36–0.55 |
| Fair | 0.40–0.69 | 0.56–0.75 |
| Poor | 0.20–0.39 | 0.76–0.90 |
| Very poor | ⩽0.19 | ⩾0.90 |

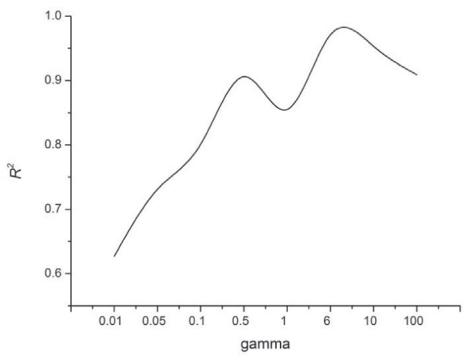


(a) The results of various *gamma* in which $C = 100$ and $\varepsilon = 0.005$.

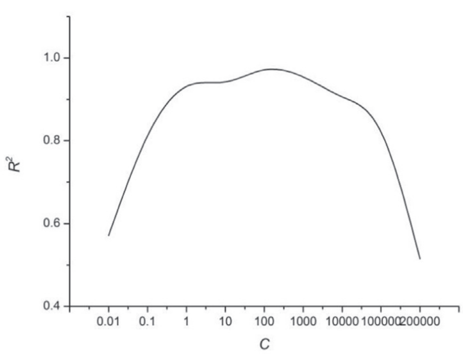


(b) The results of various $C$ in which $gamma = 6$ and $\varepsilon = 0.005$.

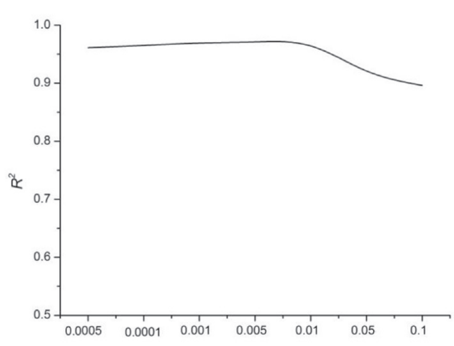


(c) The results of various ε in which $C = 100$ and $gamma = 6$.

Fig. 2. Sensitivity of the $R^2$ to SVM model control parameters ($C$, ε and *gamma*).

fixed at 100 and 0.005. The figure shows that the $R^2$ on the training set increases initially but subsequently fluctuates with *gamma* increases. An appropriate value for *gamma* would be between 1 and 10. In this aspect, it can be said that *gamma* plays an important role on the generalization performance of SVMs. Fig. 2b gives the results of various $C$ where *gamma* and ε are, respectively, fixed at 6 and 0.005. It can be observed that the $R^2$ on the training set increases initially but subsequently decreases monotonically as $C$ increases. Fig. 2c gives the results of SVMs with various ε where *gamma* and $C$ are, respectively, fixed at 6 and 100. Fig. 2c shows that the $R^2$ on the training set is very comparatively stable and relatively unaffected by changes in ε. This indicates that the performance of SVMs is insensitive to ε. However, the number of support vector decreases as ε increases, especially when ε is larger than 0.01 [33].

## 4. Results and discussion

To verify the satisfactory performance of the training process, the SVM model is used to predict the autogenous shrinkage of concrete mixtures from the training data set using the eight input variables. The plot of statistical analysis is presented in Fig. 3a. The figure includes the equity line as a reference, which represents the condition of equal values for the predicted and measured autogenous shrinkage strains. The points are mostly located on or slightly under/above the equity line between the experimental and predicted expansion values. It was demonstrated that the SVM model captured the input-output relationships exactly. The RMSE, $R^2$, and $S_e/S_y$ values were 23.14 με, 0.971, and 0.174, respectively, which indicate that the performance of the SVM is satisfactory.

The generalization capacity of the SVM was examined by testing the testing data (20% of the original database). Results of statistical analysis for the testing data are presented in Fig. 3b. As mentioned previously, the test vectors form an independent data set, which were not previously presented to the model, and thus the predictive capacity of the model for new data can be evaluated. The value of $R^2$ that evaluates the performance of the model in predicting the autogenous shrinkage values scattered around the line of equality without bias is found to be 0.924. And the *RMSE* and $S_e/S_y$ values were found to be 33.29 με and 0.286, respectively. It can be deduced that the SVM had a satisfactory generalization capacity for predicting the autogenous shrinkage of similar concrete mixtures exposed.

As for validation data set, the results of statistical analysis for the validation data are presented in Fig. 3c. The RMSE, $R^2$, and $S_e/S_y$ values were 31.15 με, 0.948, and 0.239, respectively, indicating excellent performance of the SVM model.

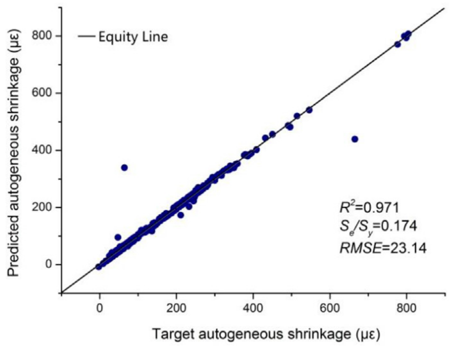


(a)Training

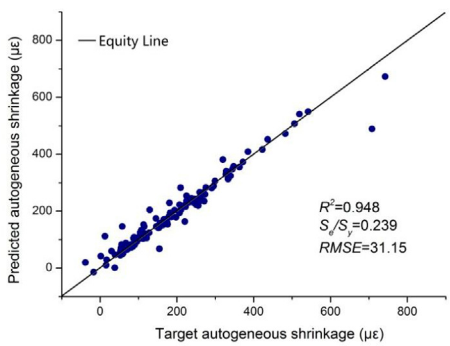


(b)Validation

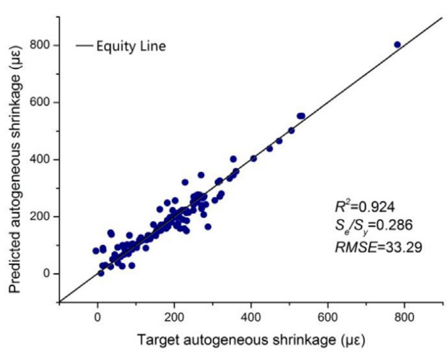


(c)Testing

Fig. 3. Response of SVM model in predicting autogenous shrinkage of concrete: (a) training; (b) validating; and (c) testing.

The accuracy of the proposed SVM autogenous shrinkage model was compared with the ANN based predictive model. Details related to the development and performance of the selected ANN autogenous shrinkage model are described in Nehdi and Soliman (2012) [18]. The plus-minus sign of autogenous shrinkage used in Nehdi and Soliman (2012) [18] is opposite to this study. Results of the statistical analysis of the ANN model are presented in Fig. 4 for the testing data points. The predictions of ANN models show slightly higher $R^2$ value compared to that of SVM model, but the *RMSE* obtained using SVM is almost one-half that of ANN model. Results of this comparison indicate that the prediction performance of SVM is comparable to ANN, although not as good. Nevertheless, the SVM has many advantages over the ANN. For

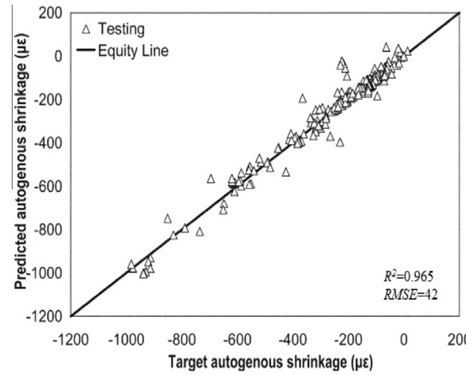


Fig. 4. Response of ANN model in predicting autogenous shrinkage of concrete for testing data [18].

instance, the development of ANN model requires a large number of controlling parameters for optimization and a relatively large training database while SVM require only three controlling parameters ($C$, ε, and *gamma*) with little dependency on the magnitude of training data sets required. These advantages of SVM can make it a promising alternative to ANN.

## 5. Validating SVM model using experimental work

### 5.1. Material

P·O42.5 type Portland cement having specific gravity of 3.14 and Blaine fineness of 327 $m^2$/kg was utilized in this study, Its chemical composition are given in Table 4, and the information was provided by the cement supplier.

The coarse aggregate used was crushed granite with a nominal size of 5–16 mm, and the fine aggregate used was river sand with a fineness modulus of 2.3. The specific gravity for the coarse and fine aggregates was 2.66 and 2.65 respectively. The grading of the aggregates was kept constant for concrete production.

A naphthalene-based superplasticizer was used in this study, its water-reducing rate is beyond 20%.

### 5.2. Mixture proportions

Mixture proportions of the concrete studied are given in Table 5. The w/c ratio of the concrete ranged from 0.3 to 0.5.

### 5.3. Specimen preparation and test method

The concrete was mixed in a laboratory pan mixer. The fine and coarse aggregates were mixed first, followed by the addition of cement. After the materials were uniformly dispersed, water and the HRWRA were added and mixed together until a consistent mixture was obtained.

In order to measure the length change of concrete, the method similar to the one applied by Lee et al. [36] was used, as shown in Fig. 5. For each mixture, two concrete

Table 4
Chemical composition of cement.

| Composition | CaO | $SiO_2$ | $Al_2O_3$ | $Fe_2O_3$ | $SO_3$ | MgO | $K_2O$ | $Na_2O$ | LOI | Free CaO |
|---|---|---|---|---|---|---|---|---|---|---|
| Proportion(%) | 64 | 21.1 | 4.9 | 3.0 | 2.1 | 1.6 | 0.78 | 0.18 | 2.1 | 0.95 |

Table 5
Mix proportions for concrete.

| Mix ID | Mix proportions (kg/m$^3$) | | | | | w/cm | TA(%) |
|---|---|---|---|---|---|---|---|
| | Cement | Water | Sand | Coarse aggregate | HRWRA | | |
| LJ1 | 382 | 191 | 641 | 1190 | 0 | 0.5 | 65% |
| LJ2 | 409 | 184 | 635 | 1176 | 0.6% | 0.45 | 65% |
| LJ3 | 439 | 175 | 625 | 1162 | 0.8% | 0.4 | 65% |
| LJ4 | 481 | 168 | 612 | 1139 | 1.0% | 0.35 | 65% |
| LJ5 | 531 | 159 | 597 | 1109 | 1.2% | 0.3 | 65% |

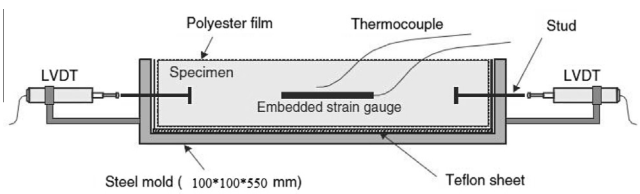


Fig. 5. Experimental set-up for autogenous shrinkage test.

prisms of 100 × 100 × 550mm were prepared. Before the removal of the mold, two LVDTs contacted on the stud and an embedded strain gauge positioned at the center of the specimen were installed to monitor the length change of the specimen. A thermocouple was also embedded horizontally in the center of the prism. The molded specimens were covered with polyester films to prevent moisture loss. Immediately after demolding, specimens were wrapped with aluminum adhesive tape. The temperature of each concrete prism used for determining the autogenous shrinkage was recorded by the thermal couple embedded. All specimens were stored in a chamber at a 20 ± 2 °C and a relative humidity of 50 ± 5% during the test.

### *5.4. Discussion of experimental results*

Fig. 6 shows the tendencies of the autogenous shrinkage values obtained from experimental study and proposed SVM model. It can be observed that the SVM predictions are in relatively good agreement with the measured results. Fig. 7 presents the comparison between the measured and SVM model predicted autogenous shrinkage values, The RMSE, $R^2$, and $S_e/S_y$ values were 47.36 με, 0.906, and

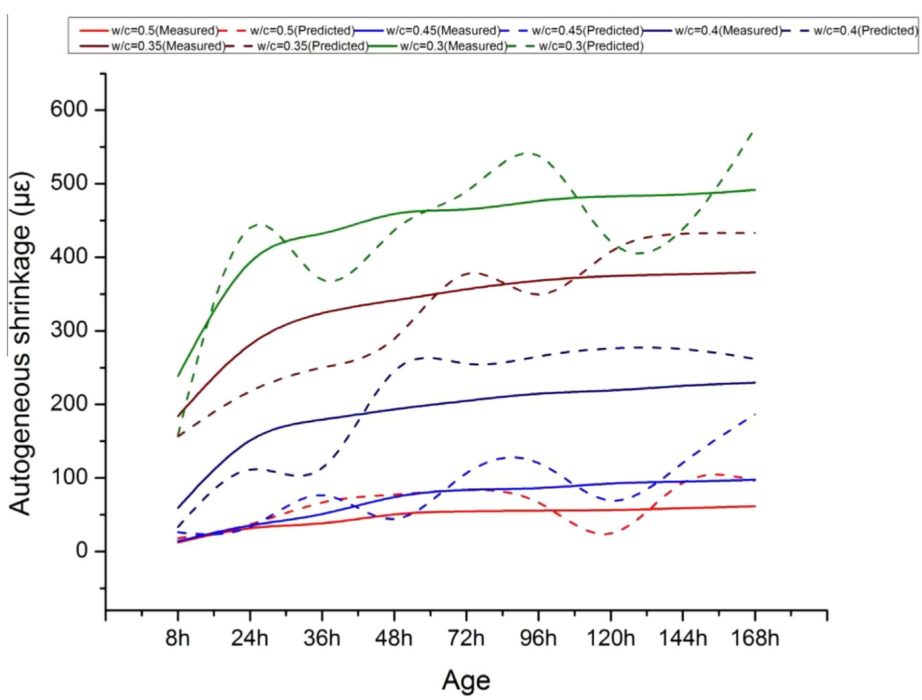


Fig. 6. Measured autogenous shrinkage values compared with predicted values.

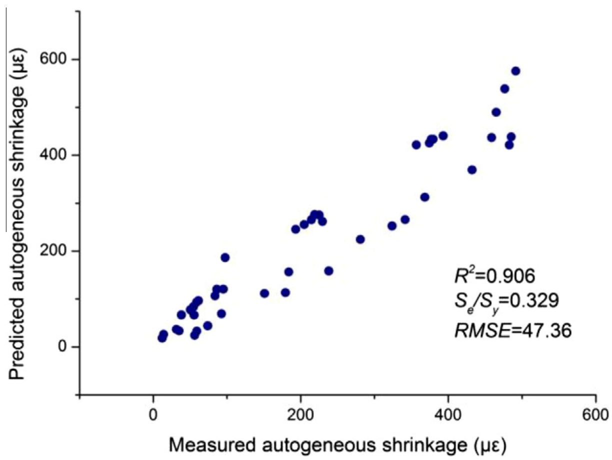


Fig. 7. Predicted versus observed autogenous shrinkage values of SVM model.

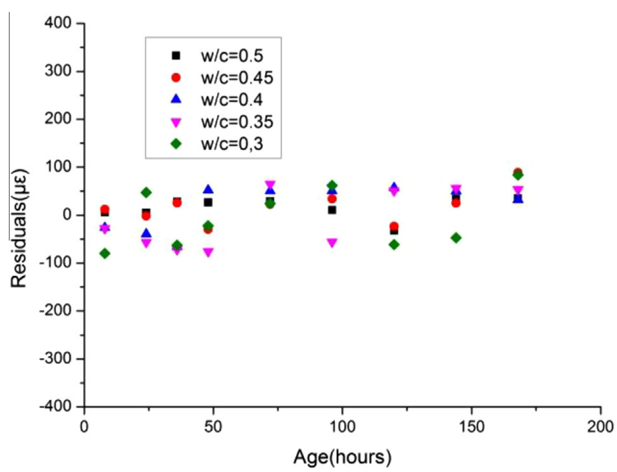


Fig. 8. Residual values for SVM model predictions.

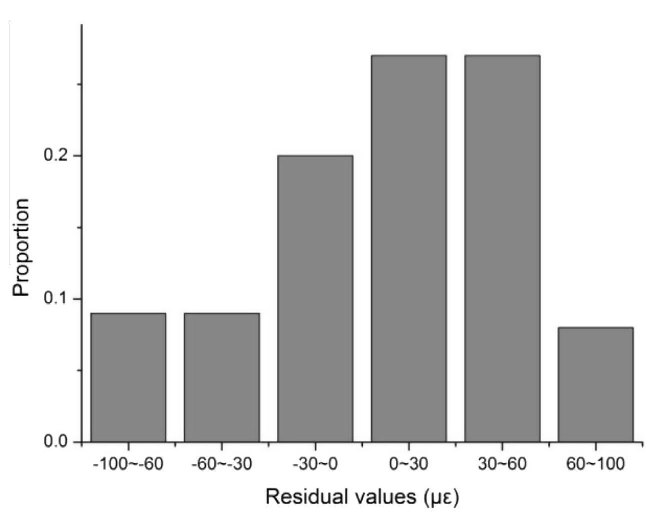


Fig. 9. Proportion of different residual value ranges.

0.329, respectively, which indicates that the SVM is able to provide prediction of the autogenous shrinkage of similar concrete mixtures.

Residual value (predicted values subtract measured values) was applied to evaluate the performance of the proposed SVM model. The residuals of tested mixtures are plotted in Fig. 8. Positive residuals indicate that the model underestimated the autogenous shrinkage, and negative residuals indicate that the model overestimates them. It is clear that almost all of residuals are within a range of ±100 με, which indicates a reasonable performance of the SVM model. Besides, as shown in Fig. 9, the distributions of the residuals in the positive region are greater than that in the negative range, indicating that the SVM model slightly underestimated autogenous shrinkage.

## 6. Conclusions

Autogenous shrinkage is a highly complex mechanism that makes modeling its behavior a difficult task. This study has proposed using an SVM model to predict autogenous shrinkage of concrete mixtures, in order to examine the applicability and potential of SVM in characterization of construction materials. The data used to develop the SVM model were from the existing literature. A comprehensive sensitivity analysis of SVM control parameters ($C$, $\varepsilon$ and *gamma*) on the $R^2$ of the SVM based predictive autogenous shrinkage models was conducted. The *gamma* and $C$ play an important role in the generalization performance of SVMs and the performance of SVMs is insensitive to $\varepsilon$. The developed SVM model was compared with the ANN-based model. It was found the prediction performance of SVM is comparable to the ANN. However, development of ANN model requires a large number of controlling parameters while the SVM model is relatively easy. The developed SVM model was validated using experimental work. It was found that the SVM model is a viable method for predicting autogenous shrinkage strains of concrete and the SVM model slightly underestimated autogenous shrinkage. Nevertheless, the proposed SVM model is restricted to extrapolation within the domain of the data used in its training. Furthermore, a more comprehensive database may increase the prediction accuracy. Also, the prediction accuracy may further be enhanced by including other experimental variables.

## References

[1] M.J. Oliveira, A.B. Ribeiro, F.G. Branco, Combined effect of expansive and shrinkage reducing admixtures to control autogenous shrinkage in self-compacting concrete, Constr. Build. Mater. 52 (2) (2014) 267–275.
[2] B. Craeye, M. Geirnaert, G.D. Schutter, Super absorbing polymers as an internal curing agent for mitigation of early-age cracking of high-performance concrete bridge decks, Constr. Build. Mater. 25 (1) (2011) 1–13.
[3] S. Ghourchian, M. Wyrzykowski, P. Lura, M. Shekarchi, B. Ahmadi, An investigation on the use of zeolite aggregates for internal curing of concrete, Constr. Build. Mater. 40 (3) (2013) 135–144.
[4] C.G. Lyman, Growth and Movement in Portland Cement Concrete, Oxford University Press, London, UK, 1934, pp. 1–139.

[5] A. Radocea, Autogenous volume change of concrete at very early age, Mag. Concr. Res. 50 (2) (1998) 107–113.
[6] T.H. Wee, S.N. Lim, Autogenous shrinkage of ground-granulated blast-furnace slag concrete, ACI Mater. J. 97 (5) (2000) 587–593.
[7] M.H. Zhang, C.T. Tam, M.P. Leow, Effect of water-to-cementitious materials ratio and silica fume on the autogenous shrinkage of concrete, Cem. Concr. Res. 33 (10) (2003) 1687–1694.
[8] C. Jiang, Y. Yang, Y. Wang, Y. Zhou, C. Ma, Autogenous shrinkage of high performance concrete containing mineral admixtures under different curing temperatures, Constr. Build. Mater. 61 (3) (2014) 260–269.
[9] E. Tazawa, Autogeneous shrinkage caused by self desiccation in cementitious material, Int. Cong (1992) 712–718, On the Chemistry of Cement New Delhi.
[10] P.C. Aitcin, A.M. Neville, P. Acker, Integrated view of shrinkage deformation, Concr. Int. 19 (1997).
[11] S. Mak, D. Ritchie, A. Taylor, R. Diggin, Temperature effects on early age autogenous shrinkage in high performance concretes, in: E. Tazawa (Ed.), Autogenous Shrinkage of Concrete: Proceedings of the International Workshop, Japan Concrete Institute, Taylor & Francis, 1999, pp. 155–166.
[12] E.I. Tazawa, S. Miyazawa, T. Kasai, Chemical shrinkage and autogenous shrinkage of hydrating cement paste, Cem. Concr. Res. 25 (2) (1995) 288–292.
[13] ACI Committee 209, Prediction of creep, shrinkage, and temperature effects in concrete structures, Aci Special Publication, 1992.
[14] CEB-FIP 1990, Model Code for concrete structures, Bull. Inf. 199 (1991) 201.
[15] N.J. Gardner, M.J. Lockman, Design provisions for drying shrinkage and creep of normal-strength concrete, ACI Mater. J. 98 (2) (2001) 159–167.
[16] ACI Committee 209, Guide for Modeling and Calculating Shrinkage and Creep in Hardened Concrete (ACI 209.2R-08), American Concrete Institute, Farmington Hills, MI, 2008, pp. 44.
[17] V. López, A. Pacios, Modelling the influence of sra on properties of hpc, Measuring Monit. Model. Concr. Prop. (2006)
[18] M. Nehdi, A.M. Soliman, Artificial intelligence model for early-age autogenous shrinkage of concrete, ACI Mater. J. 109 (3) (2012) 353–362.
[19] K. Yan, C. Shi, Prediction of elastic modulus of normal and high strength concrete by support vector machine, Constr. Build. Mater. 24 (8) (2010) 1479–1485.
[20] Y.B. Dibike, D. Solomatine, S. Velickov, M.B. Abbott, Model induction with support vector machines: introduction and applications, J. Comput. Civil Eng. 15 (3) (2014) 208–216.
[21] S.H. An, U.Y. Park, K.I. Kang, M.Y. Cho, H.H. Cho, Application of support vector machines in assessing conceptual cost estimates, J. Comput. Civil Eng. 21 (4) (2007) 259–264.
[22] M.K. Gill, T. Asefa, M.W. Kemblowski, M. Mckee, Soil moisture prediction using support vector machines, Jawra J. Am. Water Resour. Assoc. 42 (4) (2007) 1033–1046.
[23] H.B. Zhao, Slope reliability analysis using a support vector machine, Comput. Geotech. 35 (3) (2008) 459–467.
[24] P. Samui, Support vector machine applied to settlement of shallow foundations on cohesionless soils, Comput. Geotech. 35 (3) (2008) 419–427.
[25] K.C. Lam, E. Palaneeswaran, C.Y. Yu, A support vector machine model for contractor prequalification, Autom. Constr. 18 (2) (2009) 321–329.
[26] A.T.C. Goh, S.H. Goh, Support vector machines: their use in geotechnical engineering as illustrated using seismic liquefaction data, Comput. Geotech. 34 (5) (2007) 410–421.
[27] V. Vapnik, A. Chervonenkis, V. Vapnik, A. Chervonenkis, A note on one class of perceptrons, Autom. Remote Control 25 (1964).
[28] V. Vapnik, The Nature of Statistical Learning Theory, Springer, New York, 1995.
[29] S.R. Gunn, Support vector machines for classification and regression, Technical Rep., Image Speech and Intelligent Systems Research Group, Univ. of Southampton, Southampton, U.K, 1998.
[30] A. Smola, B. Scholkopf, A tutorial on support vector regression, Stat. Comput. 14 (2004) 199–222.
[31] K. Gopalakrishnan, S. Kim, Support vector machines approach to HMA stiffness prediction, J. Eng. Mech. 137 (2) (2014) 138–146.
[32] T.K. Pellinen, Investigation of the Use of Dynamic Modulus as an Indicator of Hot-Mix Asphalt Performance thesis (Ph.D.), Arizona State University, Tempe, AZ, 2001.
[33] F.E.H. Tay, L. Cao, Application of support vector machines in financial time series forecasting, Omega 29 (4) (2001) 309–317.
[34] S.I. Igarashi, A. Bentur, K. Kovler, Autogenous shrinkage and induced restraining stresses in high-strength concretes, Cem. Concr. Res. 30 (11) (2000) 1701–1707.
[35] Y. Yang, R. Sato, K. Kawai, Autogenous shrinkage of high-strength concrete containing silica fume under drying at early ages, Cem. Concr. Res. 35 (3) (2005) 449–456.
[36] K.M. Lee, H.K. Lee, S.H. Lee, G.Y. Kim, Autogenous shrinkage of concrete containing granulated blast-furnace slag, Cem. Concr. Res. 36 (7) (2006) 1279–1285.
[37] B. Akcay, M.A. Tasdemir, Optimisation of using lightweight aggregates in mitigating autogenous deformation of concrete, Constr. Build. Mater. 23 (1) (2009) 353–363.
[38] M. Sah, R. Sato, Effect of curing methods on autogenous shrinkage and self-induced stress of high-performance concrete, ACI Mater. J. 107 (1) (2010) 65–74.
[39] M. Mazloom, A.A. Ramezanianpour, J.J. Brooks, Effect of silica fume on mechanical properties of high-strength concrete, Cem. Concr. Compos. 26 (03) (2004) 347–357.
[40] Y. Akkaya, C. Ouyang, S.P. Shah, Effect of supplementary cementitious materials on shrinkage and crack development in concrete, Cem. Concr. Compos. 29 (2) (2007) 117–123.
[41] A. Bentur, S.I. Igarashi, K. Kovler, Prevention of autogenous shrinkage in high-strength concrete by internal curing using wet lightweight aggregates, Cem. Concr. Res. 31 (11) (2001) 1587–1591.
[42] D. Cusson, T. Hoogeveen, Internal curing of high-performance concrete with pre-soaked fine lightweight aggregate for prevention of autogenous shrinkage cracking, Cem. Concr. Res. 38 (6) (2008) 757–765.
[43] S.W. Yoo, S.J. Kwon, H.J. Sang, Analysis technique for autogenous shrinkage in high performance concrete with mineral and chemical admixtures, Constr. Build. Mater. 34 (3) (2012) 1–10.
[44] L. Yun, S.T. Yi, M.S. Kim, J.K. Kim, Evaluation of a basic creep model with respect to autogenous shrinkage, Cem. Concr. Res. 36 (7) (2006), 1268-1268.